2019

Electronic and Geometric Structure of AlnOm and AlnOm +

Albert R. Armstrong
Virginia Commonwealth University

Electronic and Geometric Structure of

$$Al_nO_m and Al_nO_m^+$$

A thesis submitted in partial fulfillment of the requirements for the degree of Master of Science at Virginia Commonwealth University

by

Albert Roemello Armstrong

B.S. Physics, 2017

Virginia Commonwealth University

M.S. Physics and Applied Physics, 2019

Virginia Commonwealth University

Director: Dr. Shiv N. Khanna

Commonwealth Professor

Department of Physics

Virginia Commonwealth University

Richmond, VA

May 2019

Acknowledgements

I would like to start by thanking my advisor Professor Shiv Khanna for giving me the opportunity to be a part of his world renowned group. His joyful disposition and encouraging attitude had made the time I have spent conducting this research a time I will never forget. I am very grateful for the guidance he has provided as i completed this degree. I would also like to thank Dr. Arthur Reber who went above and beyond in his efforts to assist my understanding of this field. Dr. Reber has been an excellent teacher who was always there to provide insights and assistance. Without his guidance, the past two years could not have been a success. Dr. Vikas Chauhan has given wonderful guidance, and I thank him for spending his time instructing me, especially in all things

Linux. Dr. Bishop who has taught the majority of my physics classes in graduate, and spent countless imparting their knowledge onto me. I would also like to thank Dr. Riener who over that past two years has provided invaluable advice in regards to my future in science. Outside of academia, I would like to thank my family and friends for their unwavering support and faith in me.

Contents

List of Figures

Abstract

Generally, the electronic stability of aluminum clusters is associated with either closed electronic shells of delocalized electrons, or aluminum in the +3 state. To explore alternative routes for electronic stability in aluminum oxide clusters, theoretical methods were used to examine the geometric and electronic structure of Al_nO_m $(2 \leq n \leq 7; 1 \leq m \leq 10)$ clusters. Two types of electronically stable clusters with large HOMO-LUMO gaps were identified the first being $Al_{2n}O_{3n}$ clusters with a +3 oxidation state on the aluminum, and the second being planar clusters such as Al_4O_4, Al_5O_3, Al_6O_4 and Al_6O_5. The structures of the planar clusters have external Al atoms bound to a single O atom. Their electronic stability can be explained by the multiple valence Al sites with the internal

Al atoms having an oxidation state of +3, while the external Al atoms have an oxidation state of +1. The formation of $Al_nO_m^+$ clusters with high concentrations of oxygen were found experimentally. To determine the stability of such clusters theoretical methods were used to examine the geometric and electronic structure of these clusters ($2 \leq n \leq 7; 1 \leq m \leq 10$). The structures were found to be below average in terms stability, implying formation in a low collision environment.

Chapter 1

Introduction

1.1 Motivation

Aluminum oxide, commonly referred to as Al_2O_3 or alumina, is a material that plays a vital role in many processes. Although the most noted uses of alumina are as a catalyst or catalyst supports there has been evidence that this substance can also be used to create improved hydrogen fuel cells [17]. In this scenario small alumina clusters or thin films react with water to produce hydrogen. Unlike the current methods to produce hydrogen this method does not depend on fossil fuels and achieves relatively high hydrogen storage capacity while still

keeping prices low. The formation of aluminum oxides can also be a hindrance to the testing and development of some technologies. In the case of test reactors, it is not uncommon to use aluminum alloys as fuel cladding. This cladding reacts with oxygen producing an aluminum oxide film that lowers fuel performance with an inverse relation to the films thickness[18].Polarimetry is a technique commonly used in astronomical settings for measuring optical activity as each optical component in a telescope effects the polarization of the incoming light [37].In the case of aluminum mirrors understanding the polarization due to the mirror has proven to be particularly difficult. The reason for this is that after the creation of the mirror an aluminum oxide film forms, growing in thickness over several days [26]. There has alos been evidence to suggest that Al_nO_m plays a role in atmospheric chemistry[36].As aluminum oxide presents itself across a multitude of fields a fundamental understanding of the material and its many variants is of the utmost importance.

1.2 Aluminum Oxides

Aluminum oxide exists in a variety of states with the most common and thermodynamically stable form being α-Al2O3. In this form O atoms form hexagonal closed-packed planes with Al atoms occupying two of three octahedral sites between these planes. In bulk form, there also exists two metastable states, γ-Al2O3 and δ-Al2O3. In these states the Al atoms may insert themselves into tetrahedral sites [20].Along with these three forms of bulk Al2O3 there are also thin-films as discussed in the motivation section. These thin films have a mixture of 4-fold, 5-fold, and 6-fold coordination. In general, Alumina has a preference for Al atoms to exist in the +3 oxidation state while O atoms exist in the -2 oxidation state. In addition to these large scale forms of aluminum oxide there exist another set of possible forms for Aluminum-Oxide, namely clusters. At the nanoscale compounds can exist that are far removed from the 2:3 ratio generally expected for aluminum oxides. In this regime compounds with mixed valence provide a way of

stabilizing these unusual stoichiometries and may lead to unusual properties due to a decrease in the degree of charge transfer between atoms [14, 15, 23, 24, 34, 31]. Previous works have indicated that it is possible for aluminum oxide to adopt radically different structural motifs, and when supported on certain substrates can even form wide-band gap materials. . Although aluminum oxides prefer a 2:3 ratio of Al atoms to O atoms, the ground state occupation of Al provides a potential alternative. The ground state of an Al atom is $[Ne]3s^2 3p^1$ and the separation between the 3s and 3p shells is roughly 3.6 eV. As a result of this large gap there is a possibility that electronically stable structures with Al atoms in the +1 oxidation state can exist. Metalliod clusters have been formed using compounds such as Al-cyclopentadiene and Al-halides indicating that aluminum in the +1 oxidation state may be stabilized [11, 16, 44, 43, 1, 10] These results posit the question as to whether it is possible to have other stable Al_nO_m compositions that are electronically and energetically stable.

1.3 Summary and Thesis Layout

The purpose of this thesis is twofold; the first aim is to understand the stability and structural motifs of $Al_nO_m^+$ clusters in an effort to better explain experimental results. The second is to explore the structure and stability of Al_nO_m clusters while attempting to shed light on the existence and stability of planar mixed oxidation state Al_nO_m clusters. Using an ab initio approach, the Amsterdam Density Function code is used to evaluate both the stability and the structure of such clusters. The second chapter of this thesis will provide an abridged history of Density Functional Theory starting with the work of Kohn and Sham. Chapter two also serves to give pertinent specifics about the computational work carried out as well as a brief explanation of approaches taken in support of the stated purpose of this work. A brief outline of the experimental techniques used by the collaborator is given in Chapter 3. The results of the computational work in this thesis is laid out in chapters 4 and 5. Chapter four focuses on the

structure and stability of Al_nO_m with special interest given to planar structures of mixed oxidation states while chapter 5 is a study of the stability of $Al_nO_m^+$ and its relationship to the experimental studies outlined in chapter 3. Any supplemental information for chapters 4 and 5 can be found in the appendix section of this thesis.

Chapter 2

Theoretical Methods

2.1 An Introduction to Density Functional Theory

Density Function Theory is integral to the studies carried out in this thesis. The fundamental concepts of DFT and rooted in Quantum Mechanical Theory and in specific Schrodinger's equation. Although the developments of the Born-Oppenheimer approximation and the Hartee- Flock method played an integral role in the creation of modern DFT these concepts will not be discussed in detail here. This section will begin with the with the electron density proposed by

Kohn, Hohenburg, and Sham in the 1960's. They proposed that the electron density can be written as

$$n(\overrightarrow{r}) = N \int r d_2^3 \int d^3 r_3 ... \int d^3 r_N \Psi(\overrightarrow{r_1}, \overrightarrow{r_2} ... \overrightarrow{r_N}$$

From this electron density the potential of a many body system can be constructed into a single body calculation. To do such $n(\overrightarrow{r})$ is treated as a variable. As a result, other observables can be found. Once the particle density has been found this value can be used to calculate the ground state wavefunction and potential energy of the system.

Early methods attempted to directly minimize the energy of many body systems. In 1965 Kohn and Sham derived a way to do this indirectly [19]. Starting with ground state energy of an interacting inhomogeneous electron gas in a static potential

$$E = \int v(\overrightarrow{r}) n(\overrightarrow{r}) d\overrightarrow{r} + \frac{1}{2} \int \int \frac{n(\overrightarrow{r}) n(\overrightarrow{r'})}{|\overrightarrow{r} - \overrightarrow{r'}|} d\overrightarrow{r} d\overrightarrow{r'} + G[n]$$

They then devised an approximation for G[n], the universal functional of the density. G[n] is said to be made up of a

kinetic energy term and an exchange and correlation energy. The kinetic energy term can be written as the sum of two terms in the form

$$T[n] = T_s[n] + T_C[n]$$

where $T_s[n]$ represents the energy of noninteracting particles and $T_c[n]$ represents the remainder. $T_s[n]$ cannot be found directly as a functional of $n(\overrightarrow{r})$ as a result Kohn and Sham expressed $T_s[n]$ in terms of single particle orbitals of a noninteracting system whose density is $n(\overrightarrow{r})$. Doing such leads to

$$T_s[n] = -\frac{\hbar^2}{2m}\sum_i^N d^3r\phi^*(\overrightarrow{r})\nabla^2\phi(\overrightarrow{r})$$

where $\phi(\overrightarrow{r})$ is the single particle orbital. The practicality of such an approach is that as all $\phi(\overrightarrow{r})$ are functionals of $n(\overrightarrow{r})$ $T_s[n]$ becomes and implicit functional of $n(\overrightarrow{r})$. This method

allows the exact energy functional to be written as

$$E = T_s[\phi(n)] + U_H[n] + E_{xc}[n] + V[n]$$

In this scheme $E_{xc}[n]$ is the exchange-correlation energy. While this gave a more straightforward way of dealing with the exact energy functional it does not explain how to minimize that value. The general form of the minimization is given as

$$0 = \frac{\delta E[n]}{\delta n(\overrightarrow{r})} = \frac{\delta T_s[\phi(n)]}{\delta n(\overrightarrow{r})} + \frac{\delta U_H[n]}{\delta n(\overrightarrow{r})} + \frac{\delta V[n]}{\delta n(\overrightarrow{r})} + \frac{\delta E_{xc}[n]}{\delta n(\overrightarrow{r})} + v(\overrightarrow{r}) + v_H(\overrightarrow{r}) + v_{xc}(\overrightarrow{r})$$

From the above equation it can be seen that the minimization of the energy can be written as:

$$\frac{\delta E[n]}{\delta n(\overrightarrow{r})} = \frac{\delta T_s[\phi(n)]}{\delta n(\overrightarrow{r})} + v(\overrightarrow{r}) + v_H(\overrightarrow{r}) + v_{xc}(\overrightarrow{r})$$

For this equation to have physical meaning the final three terms should be explained. The value $v(\overrightarrow{r})$ represents the external potential through which the electrons move. $v_H(\overrightarrow{r})$ is the Hartee potential and represents the self-consistant electron potential. The last term is the exchange-correlation potential.

This term is of special interest as it cannot be directly calculated and is totally dependent on the approximation made for $E_{xc}[n]$.

The above results give way to what is known as the Kohn-Sham equation.

$$[-\frac{1}{2}\nabla_i^2 + v(\overrightarrow{r}) + v_H(\overrightarrow{r}) + v_{xc}(\overrightarrow{r})]\Psi_i(\overrightarrow{r}) = E\Psi_i(\overrightarrow{r})$$

The above equation is essentially Schrodinger's equation for one electron. If all potentials are said to be equal $v_s(\overrightarrow{r})$ then the equation can be solved as if there is only one potential present. This assumption gives the equation

$$[-\frac{\hbar^2\nabla^2}{2m} + v_s(\overrightarrow{r})]\phi(\overrightarrow{r}) = \epsilon\phi(\overrightarrow{r})$$

From this $n(\overrightarrow{r})$ can be found to be

$$n(\overrightarrow{r}) = \sum_i^N f_i|\phi_i(\overrightarrow{r})|^2$$

Here, f_i is the orbital occupation. The last two equation

provide a method for minimization of the exact energy functional.

In the above discussion of the Kohn-Sham theorem it has been claimed that the exchange correlation energy cannot be directly calculated. It turns out that in the case of a uniform electron gas the exchange-correlation functional can be exactly calculated [33].This is a result of the electron density be constant at all spatial points. Although, this is an approximation it allows the Kohn-Sham equations to be used. In this scenario

$$v_{xc}(\overrightarrow{r}) = v_{xc}^{electrongas}(\overrightarrow{r})$$

By applying this approximation, one needs know only the local density; as a result, this method is known as the local density approximation (LDA). While this approximation assumes a uniform charge density within the system that is, in general, not the case. To limit the error of the LDA approach Becke introduced the general gradient approximation [3, 4].In this

method he paired the LDA correlation energy with the Hartree-Fock exchange-energy. Doing such resulted in an exchange-correlation energy that could be written as:

$$E_{xc}^{LDA}[n_{\uparrow}(\overrightarrow{r}), n_{\downarrow}(\overrightarrow{r})] = \int d^3r \epsilon_{xc}[n_{\uparrow}(\overrightarrow{r}), n_{\downarrow}(\overrightarrow{r}), \nabla n_{\uparrow}(\overrightarrow{r}), \nabla n_{\downarrow}(\overrightarrow{r})] n(\overrightarrow{r})$$

2.2 Theoretical Method in Practice

All results presented in this work were carried out using Amsterdam Density Functional code. In this method atomic orbitals are formed from Slater-type orbitals (STO) centered at each atomic site [35].These slater-type orbitals are known as basis set elements and can be described by the spherical harmonics of the orbital, and some exponential function that determines the orbitals decay over long ranges. Although other types of orbitals, such as Gaussian, can be used to approximate these basis sets STO have the benefit of accurately modeling cusp behavior and long range decay of the wavefunction [25].In this work all calculations were conducted

using the TZ2P basis set [39].TZ2P on its own does not provided relativistic effects as a result the zero-order regular approximation(ZORA) was added [39].This approximation is derived by taking the zero-order expansion of the Dirac equation [38].This is then substituted in the Kohn-Sham equation as the systems potential. The electronic orbitals are then built from a linear combination of these atomic orbitals. In this work exchange and correlation effects are included using gradient corrected density functionals, specifically GGA PBE [28].The choice of this basis set is based on previous works which have shown the functional to provide an adequate representation of the electronic structure of Al_n clusters [30]. Both studies discussed here involved clusters containing multiple Al and O atoms, as a result numerous potential structures (up to 30) were investigated. These potential structures were generated by hand and included structures that were prompted by previous works involving aluminum oxide clusters[29, 42, 13, 12, 9, 8, 27]. For each potential structure various spin configurations were examined to provide

confidence that both the ground state structure and multiplicity were properly identified.

While the proper geometry of these clusters is inherently valuable these results were intended to provide insights into the experimental results of a collaborator as well as provide an explanation for planar structures with mixed oxidation states. As a result, various markers of stability were probed. The first such marker that was examined was HOMO-LUMO gap[7](c). The HOMO-LUMO gap represents the energy separation between the highest occupied molecular orbital of a cluster and the lowest unoccupied orbital. This value is of importance as a large gap indicates that a cluster will resist accepting or donating charge and as a result is a good indication of the structure's chemical stability.

Charge analysis was then carried out. This is a method by which the net atomic charge of each atom in a cluster is calculated from the molecular charge of the system. The results of these calculations provide a fractional value measured in elementary charge units. These values highlight

the asymmetry of electrons in chemical bonds and as a result carry information about bond strength. The values can also be used as a method of comparison by which one can understand the oxidation state of a particular atom. The atom that is less electronegative will carry a negative charge as its electrons are drawn to the other atom. While various methods have been devised to examine this phenomenon, Hirshfeld charge was used for all results in this thesis. This method was chosen as each atom's charge density is weighted in such a way that the charges provide more solid physical meaning than previous methods. To obtain Hirshfeld charges, the fragments of the cluster in question must be preselected. In the case of this thesis, the fragments chosen correspond to each atom present and all calculations were done using neutral charge densities.

For both Al_nO_m and $Al_nO_m^+$ clusters the fragmentation channels were examined. This is the energy required to break an Al_nO_m cluster into a fragment containing x Al and y O atoms and another containing n-x Al and m-y O atoms. The fragmentation energies, $\Delta Frag$, for an Al_nO_m cluster were

calculated with the equation

$$\Delta Frag = E(Al_xO_y) + E(Al_{n-x}O_{y-m}) - E(Al_nO_m) \qquad (2.1)$$

where $E(Al_nO_m)$ is the total energy of the initial cluster. Calculations for $Al_nO_m^+$ clusters were carried out in much the same way yet it is important to note that as these clusters are positively charged one of the fragments must also carry a positive charge. Experimentally only charged clusters can be observed; because of this the fragmentation energies of $Al_nO_m^+$ not only gives insight into the relative stability of positively charged clusters but also serves as a metric by which to understand the stability of neutral clusters within an oxygen rich environment. For each cluster all possible fragmentation channels were examined including those that contained O_2,O_3 and Al.

The adiabatic ionization energy, or the energy required to strip a single electron from a neutral cluster, was calculated using

fully optimized structures by way of the equation

$$I.E. = E(Al_nO_m^+) - E(Al_nO_m) \tag{2.2}$$

Finally, various types of binding energies were explored. For Al_nO_m clusters the oxygen binding energies were calculated via the equation

$$E_{ob} = E(Al_nO_m) - [E(Al_nO_{m-1}) + E(O] \tag{2.3}$$

In the case of $Al_nO_m^+$ clusters, O2 binding energy was calculated using the equation

$$E_{o_2b} = [E(Al_nO_{m-2}^+) + E(O_2] - [E(Al_nO_m^+) \tag{2.4}$$

In both Eq. 2.3 and 2.4 $E(Al_nO_m)$ and $E(Al_nO_{m-y})$ represent the ground state energies of each structure respectively. While both E_{Ob} and E_{O_2b} are used to gain a clearer insight as to the stability of each cluster the usage of E_{O_2b} for $Al_nO_m^+$ clusters were chosen as it could also lend insights into the formation of clusters in the experiment performed.

Chapter 3

Experimental Methods

3.1 Laser Vaporization

Our collaborator in China prepared all clusters presented in the experimental portion of this work using laser vaporization (LaVa). In this method a high-intensity laser is focused onto a rod of the material that is to be examined [5, 40].This high-intensity beam heats the rod thereby vaporizing a portion of the material. At this point a gas is pumped into the chamber quenching the vapor allowing it to condense into clusters under vacuum. It should be noted that although the sizes of clusters produced generally follow a relatively Gaussian

distribution it is not possible to size select a specific cluster. In this specific experiment an aluminum rod was vaporized and the condensation gas used was O_2. While in general the gas used is neutral as to avoid reacting with the metallic vapor, it was the intent of this experiment to create such a reaction leading to the formation of aluminum oxide clusters.

3.2 TOFMS

Proper identification of these newly formed clusters relies on the use of a time of flight mass spectrometer such as the one pictured in figure 3.1. The first step in this process is to ionize the clusters using an ionization laser. This is necessary as only charged clusters can be properly detected. An ion beam is then directed into a chamber filled with an inert gas, typically N_2. The first portion of this chamber consists of a homogeneous electric field that serves to accelerate the clusters[5]. Each cluster of the same mass travels at a set velocity through a field free drift region until it comes into

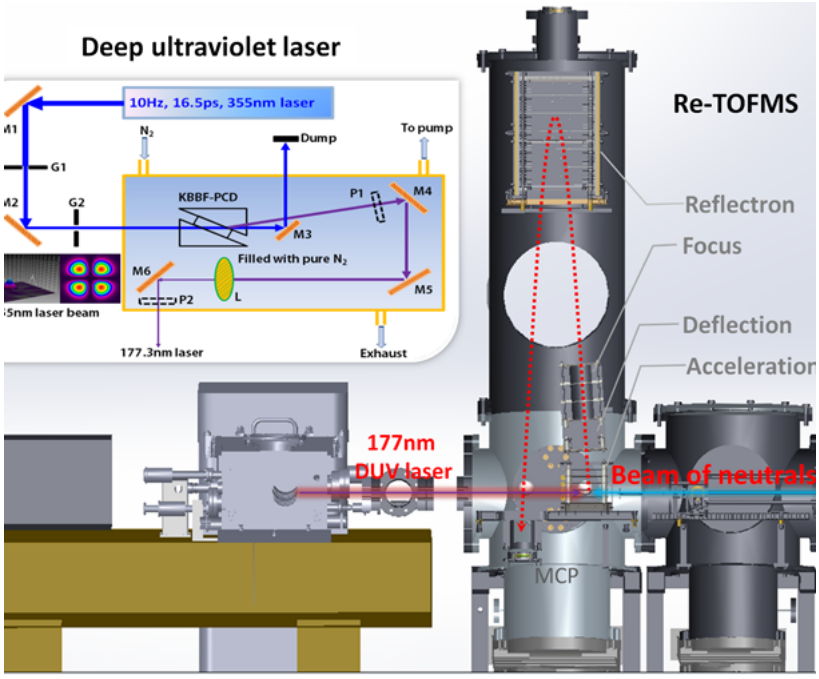

Figure 3.1: Schematic of Re-TOFMS used to charachterize $Al_nO_m^+$ clusters experimentally

contact with the detector[5].The ionization state of the cluster is controlled by the ionizing laser. This state paired with the mass of the cluster striking the detector allows for proper identification of each cluster. Although, figure 3.1 shows a deep ultraviolet laser this laser was not used in the experiment presented here. As a result this is a study of cations and not neutral structures that have simply been ionized.

Chapter 4

Structure of Al_nO_m

4.1 Geometric Structure

The ground state structures were calculated for clusters with Al from 1 to 7 and O from 1 to 10. In this work, only structures where Al is greater than 2 were considered in regards to electronic structure. The geometric structures of these clusters can be seen in figure 4.1. The two most logical constituents of an Al_nO_m cluster would be Al_2 and AlO. The calculations performed found the binding energy of Al_2 to be 1.48 eV while AlO was found to have a binding energy of 7.83 eV. From these results, one would expect that when oxygen is

brought into the presence of Al_n the oxygen will be inserted between two of the Al molecules. This can be seen in the case of Al_2O where the single oxygen molecule bonds to both Al atoms. Al_2O_2 behaves similarly, in that both oxygen atoms bind to each Al atom.After this point oxygen atoms will bond to a single Al atom until all available sites have been occupied. As these clusters become oxygen rich O-O and eventually O-O-O bonds form. For clusters where the number of Al atoms are between 4 and 6, the insertion of O atoms into more compact aluminum clusters gives rise to a region where the ground state structures are planar. These regions begin with Al_4O_2, Al_5O_3, and Al_6O_4 and terminate with Al_4O_5, Al_5O_5, and Al_6O_7. As no planar structures exist within the Al_7O_m structures it would appear that there is a size limit at which planar structures are no longer energetically favorable. An in depth discussion of the lack of planar ground states for Al_7O_m will take place in the next section.

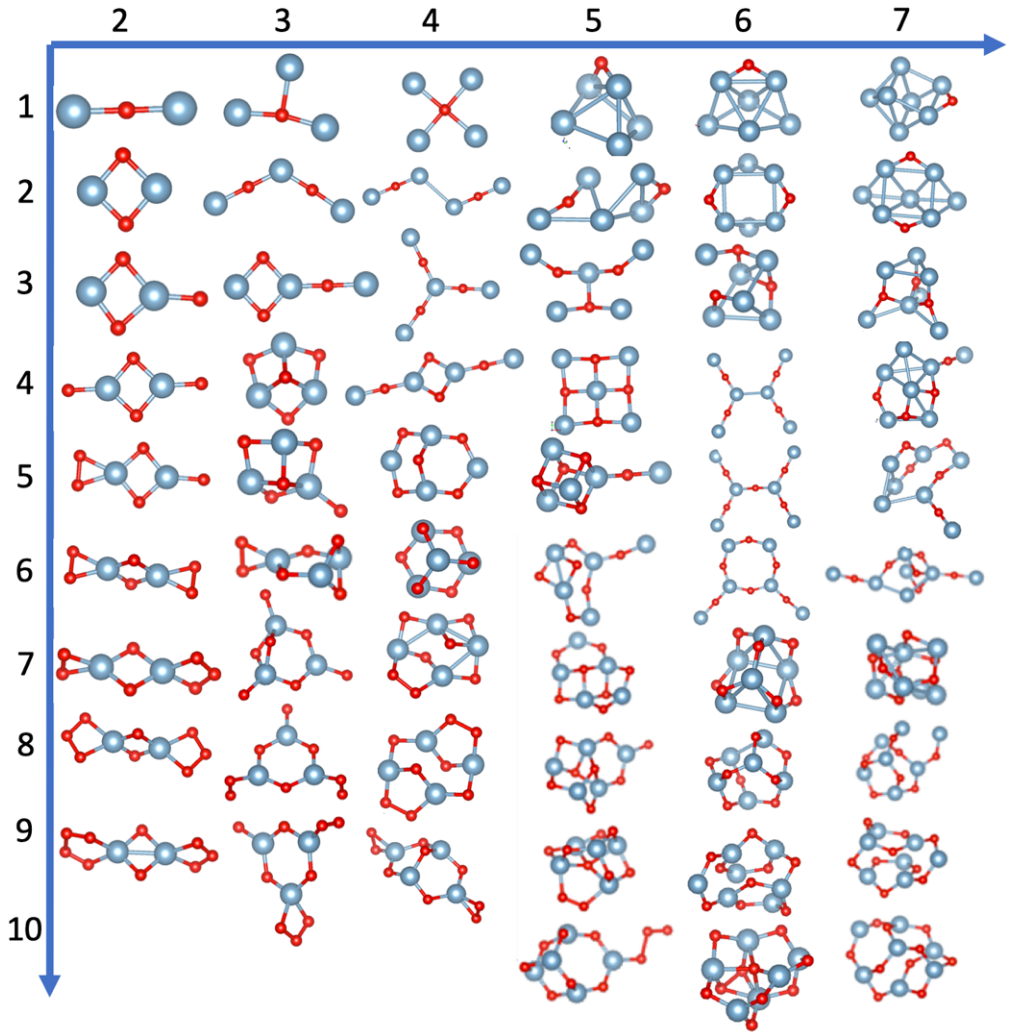

Figure 4.1: Ground-state atomic structures of Al_nO_m ($2 \leq n \leq 7; 1 \leq m \leq 10$). Aluminum is blue, Oxygen is Red.

4.2 Electronic Structure

The next stage of this work involved examination of the electronic structure of each cluster in an effort to determine the electronic stability. This was done by calculating the HOMO-LUMO gap, fragmentation energy, and oxygen binding energy of each ground state structure. Figure 4.2 gives the HOMO-LUMO gaps for the various Al_nO_m clusters. While a large HOMO-LUMO gap does not have inherent meaning, when paired with a closed electronic shell it is indicative of lowered reactivity as well as higher ionization and reduced electron affinity. From this one would expect that clusters with closed electronic shells would have higher than average HOMO-LUMO gaps. Al atoms have three valence electrons whereas oxygen six, two short of a closed shell. From this it can be seen that Al_2O_3, Al_4O_6 and Al_6O_9 will have closed electronic shells. Although these clusters were found to have quite large HOMO-LUMO gaps the largest gaps were found to belong to Al_4O_4 and Al_6O_5, with the HOMO-LUMO gaps of

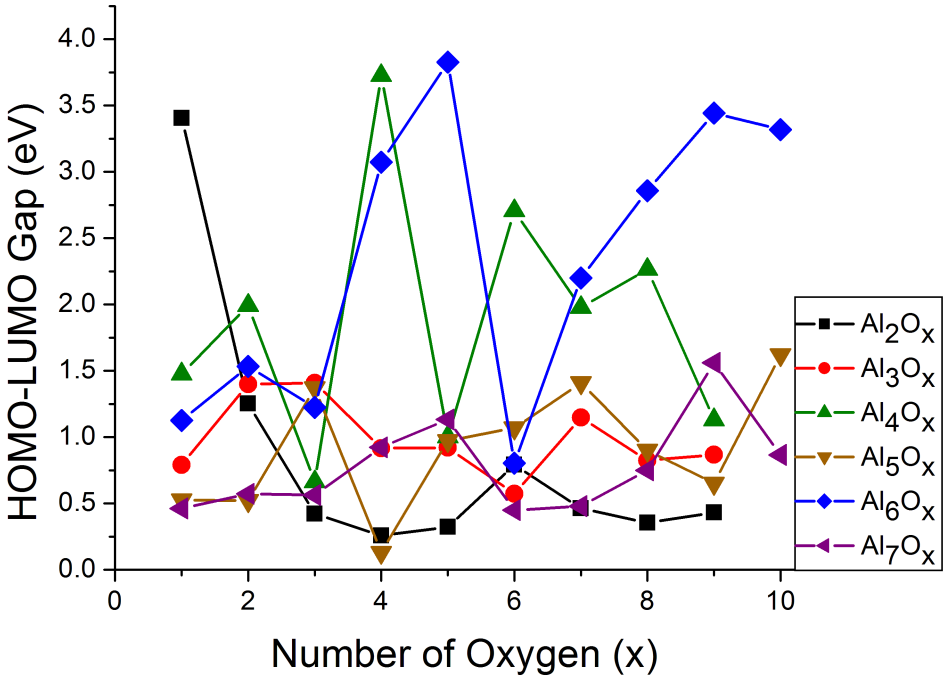

Figure 4.2: HOMO-LUMO gaps of Al_nO_m $(2 \leq n \leq 7; 1 \leq m \leq 10)$

Al_2O, Al_6O_4 and Al_6O_8 all being greater than that of Al_4O_6.

Eq. 2.1 was used to calculate the Fragmentation energies shown in figure 4.3. For the various Al contents, it was found that Al_2O, Al_3O_4, Al_4O_6, Al_5O_7, Al_6O_9, and Al_7O_{10} had the largest fragmentation energies. With the exception of Al_2O all Al_nO_m clusters where n is even correspond to an integer multiple of the 2:3 ratio found in bulk Alumina. Although, the

result that Al_2O has a larger fragmentation energy than Al_2O_3 is initially shocking, it can reasoned that as each Al atom shares one electron with the single oxygen that needs two electrons to fill its outer shell this structure would be less likely to fragment than the Al_2O_3 cluster which has its third oxygen bonded to a single Al atom. Considering the values for the HOMO-LUMO gap in conjunction with the fragmentation energies of each cluster allows one to develop a clearer understanding of these Al_nO_m clusters. Although, Al_4O_4, Al_6O_4, Al_6O_5, and Al_6O_8 all had very large HOMO-LUMO gaps their various fragmentation energies are average with regards to all Al_nO_m clusters. Al_4O_6 and Al_6O_9 on the other hand, have both large HOMO-LUMO gaps as well as the largest fragmentation energies thereby implying that these two structures are in fact more stable than the rest of the Al_nO_m clusters. Figure 4.3B charts the fragmentation energies as a function of their O/Al ratio, with the fragmentation channel highlighted by the smallest of the two fragments. The most common fragments are O_2, AlO, and Al_2O. In the case of

oxygen rich clusters, the fragmentation channel generally involves an O_2 molecule and in rare instances a single O. As the ratio of O to Al approaches 3:2 the most common fragment becomes AlO. In the cases where there are more Al atoms than O, Al_2O becomes the most common fragment followed by a single Al atom. These fragmentation trends imply that Al_nO_m clusters in fact prefer the 2:3 ratio seen in bulk Alumina.

Figure 4.4 shows the O binding energy across Al_nO_m structures. Although, fragmentation energy has already been used to discuss energetic stability and is in general a better metric to use, O binding energy gives another route by which to examine the energetic stability of clusters detailed in this work. It can be seen that the planar structures Al_4O_4, Al_6O_4, and Al_6O_5 all have above average binding energies with the O binding energy for Al_6O_4 actually surpassing that of the Al_6O_9 structure which has a stochiometry equal to Al_2O_3. While these results do not imply that fragmentation of these clusters is unlikely, the results do support that each O atom is strongly bound to Al and as a result one would expect any

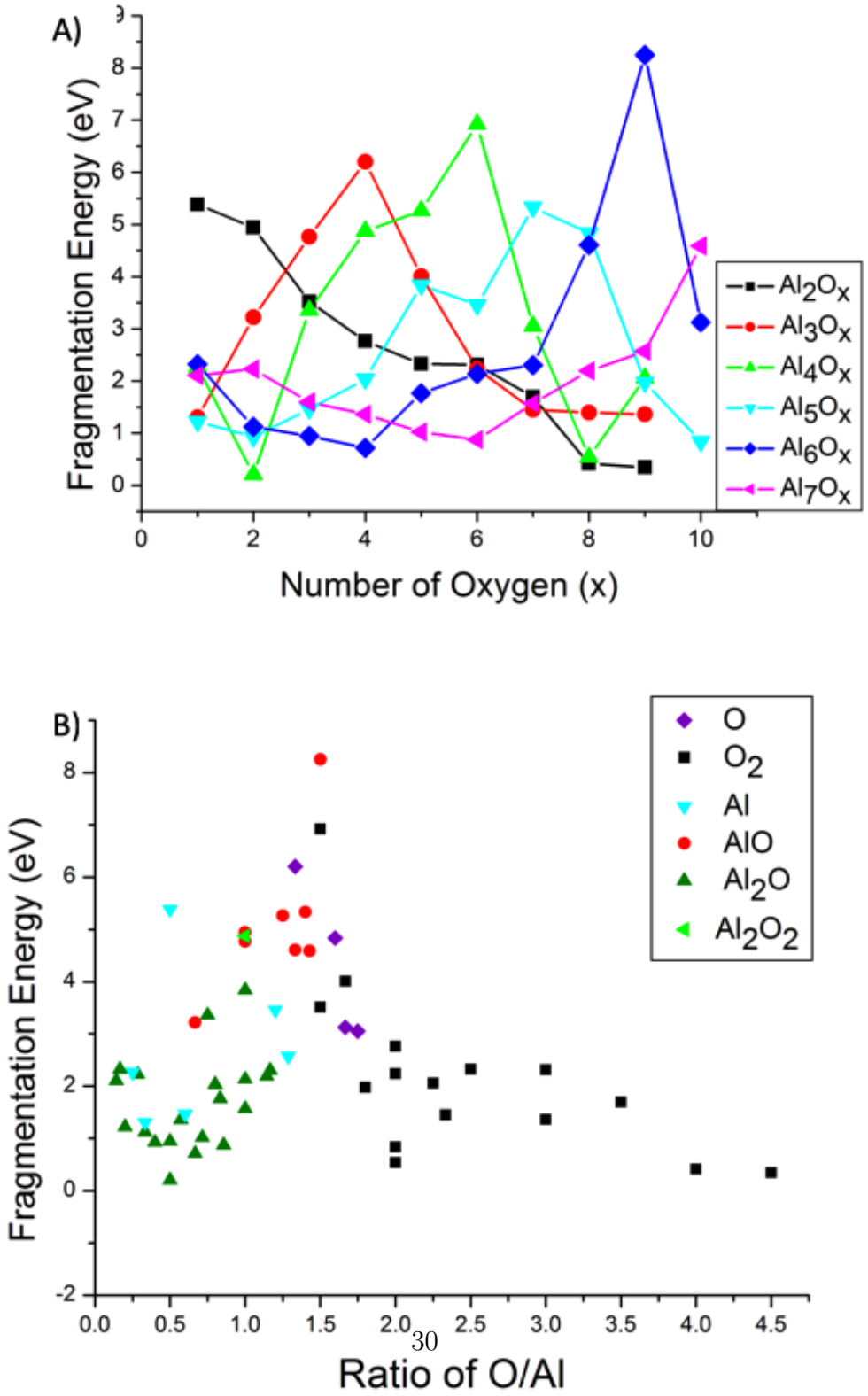

Figure 4.3: A) Fragmentation energy of Al_nO_m $(2 \leq n \leq 7; 1 \leq m \leq 10)$ B)Fragmentation energy of Al_nO_m $(2 \leq n \leq 7; 1 \leq m \leq 10)$ as a ratio of O/Al with lowest channel represented by smallest fragment.

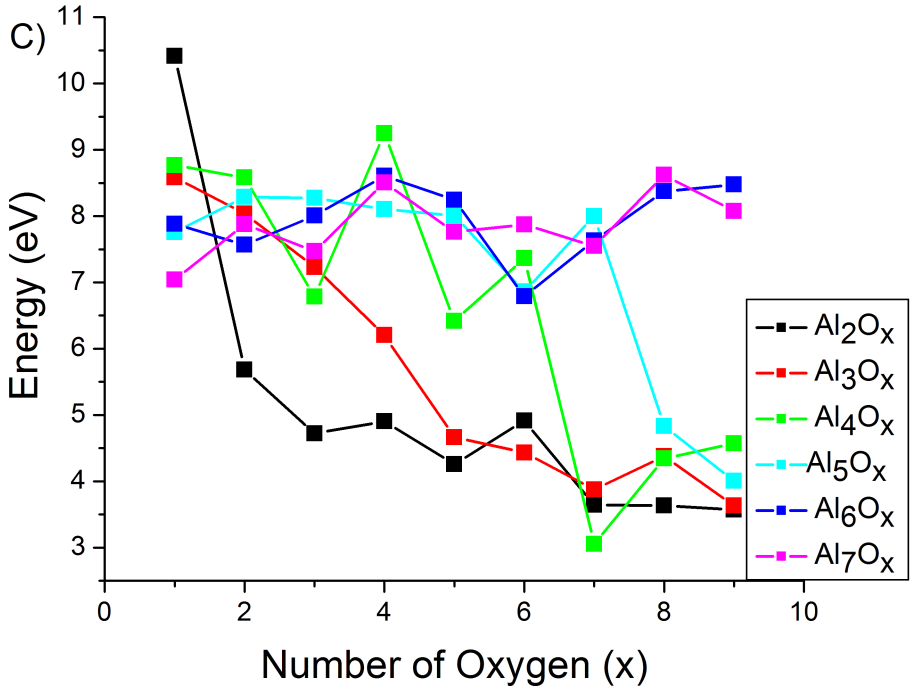

Figure 4.4: Oxygen Binding energy of Al_nO_m $(2 \leq n \leq 7; 1 \leq m \leq 10)$

fragmentation that does happen to happen along a channel in which AlO or Al_2O present. This supports the data presented in Figure 4.3B.

4.3 Electronic Structure of Planar Al_nO_m

The structures Al_4O_4, Al_6O_4, Al_6O_5, andAl_6O_6 were all found to have planar geometries. It was postulated that the

electronic stability of these structures was the result of multiple valances present on the Al atoms, and in particular the presence of terminal Al atoms in the +1 oxidation state. To confirm this claim the electronic structure of these clusters were studied in particular. In Figure 4.5 the structure, Hirshfield charge and HOMO-LUMO gap are present for Al_2O, Al_4O_4 and Al_4O_6. While Al_2O and Al_4O_6 are not planar structures their inclusion here is vital to understanding of the oxidation states of the planar clusters. By comparing the Hirshfield charge of each planar structure to the Hirshfield charges of either Al_2O or Al_4O_6 it is possible to assign an effective oxidation state to each Al atom in the planar clusters. For Al_2O the HOMO-LUMO gap was found to be 3.41 eV. This gap corresponds to the gap lying between the $3s^2$ and 3p orbitals. In this cluster the Al atoms are in the +1 oxidation state whereas the O atom is in the -2 oxidation state. The +1 oxidation state corresponds to an integrated charge of 0.23 on the Al atoms. The -2 oxidation state corresponds to an integrated charge of -0.45 on the oxygen. In the case of Al_4O_6

the HOMO-LUMO gap was found to be 2.71 eV. Although this HOMO-LUMO gap is larger than what is generally found in AlO clusters it is lower than what one expect for a cluster with a closed electronic shell. This is the result of unoccupied 3s orbitals in Al forming a bonding orbital roughly 2 eV lower than those of the other unoccupied orbitals. The Al atoms in Al_4O_6 are found to be in the +3 oxidation state whereas the O atoms are in the -2 oxidation state. The +3 oxidation state corresponds to an integrated charge of of 0.64 on the Aluminum. The -2 oxidation state corresponds to an integrated charge of -0.42. With these results in mind, Al_4O_4 can be examined.

Al_4O_4 has two central Al atoms with integrated charges of 0.61. This is essentially the same as the charges found on the Al atoms of Al_4O_6. The terminal Al atoms have charges of 0.27 which are roughly in line with those of the Al atoms in Al_2O. From these results it can be seen that the electronic stability of Al_4O_4 can be attributed to its multiple valance in the aluminum atoms. Figure 4.6 shows the structure,

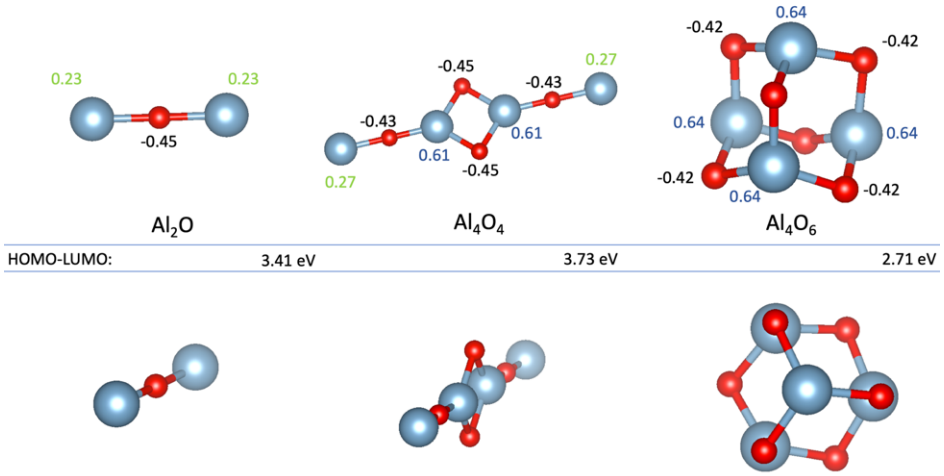

Figure 4.5: Structure of Al_2O, Al_4O_4, and Al_4O_6, HOMO-LUMO gap, and Hirshfeld charges of the atoms.

HOMO-LUMO gap, and Hirshfield charge for Al_6O_4, Al_6O_5, and Al_6O_6. Al_6O_4 is found to have a HOMO-LUMO gap of 3.07 eV. The Hirshfield charge on O is found to be -0.44 eV. The two central atoms are trivalent, forming bonds with two O atoms and one bond with another Al. These central atoms are found to have an integrated charge of 0.44. The four terminal Al are bonded to a singular O atom and have charges of 0.23. These results support the premise that each O pulls an electron from each terminal Al, leaving these terminal Al atoms in the +1 oxidation state. From these results it can also be seen that

each O atom pulls one electron from the central Al atoms leaving a single electron on each terminal aluminum by which they bind. As the terminal Al atoms are in the +1 state, they each have filled $3s^2$ shell. This paired with the trivalent nature of the central Al atoms provides a clear insight into the large HOMO-LUMO gap of Al_6O_4. Although the case for the electronic stability of Al_6O_5 could be made in much the same way as the two previous structures it is not strictly necessary to do such. In this case the terminal Al atoms each donate an electron to the nearest oxygen making the terminal Al atoms monovalent, whereas the central Al atoms will donate three electrons, one to each neighboring oxygen, leaving these atoms in the +3 state and all O in the -2 state. Although both Al_6O_4 and Al_6O_5 are perfectly planar in their ground states they are not aromatic[22, 21, 6, 32, 2, 41]. While all-metal aromatic clusters derive their stability from degeneracies caused by planar structures with delocalized electrons these clusters are stable as a result of atomic shell filling which would hold without regard to structure. The structures planarity can be

attributed to limited amounts of pi bonding between Al and O atoms. Al_6O_6 is not perfectly planar and has a HOMO-LUMO gap of 0.8 eV, substantially smaller than those of Al_6O_4 and Al_6O_5. This can be explained by noting that although the terminal Al atoms are monovalent and the top most Al atoms within the ring are trivalent, the lower two Al atoms are divalent. Examination of the Hirshfield charge supports this as the lower Al atoms have a charge of 0.44 which is intermediate of the monovalent (0.24) and trivalent (0.64) charges. Figures 4.7a and 4.7b plot the Hirshfield charge on oxygen and aluminum with respect to cluster size. This data was used to analyze the effects of oxygen coverage on the charge transfer of Al_nO_m clusters. In general O atoms have a charge between -0.4 and -0.45, although once the ratio of Al to oxygen exceeds 1:2 this no longer holds true as after that point O-O bonds begin to form. It can be seen in figure 4.7b that after Al_2O_4, Al_3O_5,Al_4O_6, Al_5O_8, Al_6O_9, andAl_7O_{10} there is a monotonic decrease in charge. This implies that after that point the cluster has reached oxygen saturation. It is also of interest

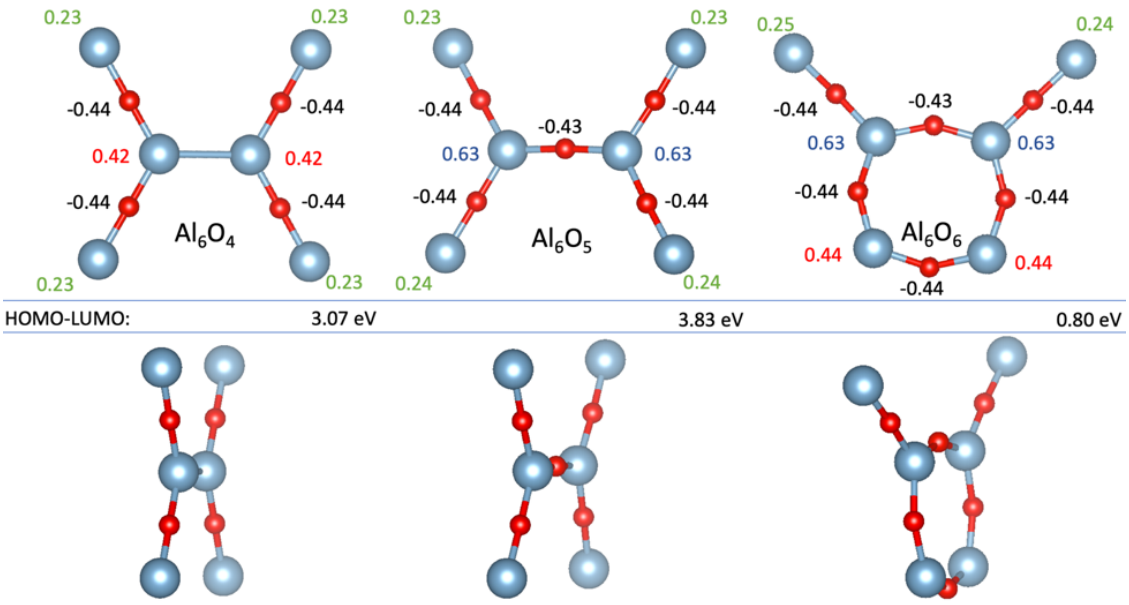

Figure 4.6: Structure of Al_6O_4, Al_6O_5, and Al_6O_6, HOMO-LUMO gap, and Hirshfeld charges of the atoms. Green corresponds to Al in the +1 valent state, blue is +3, and red is +2.

that for each value of n for Al_nO_m clusters this point occurs at approximately the 2:3 ratio of Al to O. These saturation points all occur near 0.6 which is consistent with the values associated with the +3 oxidation state.

To provide further confirmation that the terminal atoms of these planar structures are indeed monovalent, the molecular orbitals of Al_6O_4 and Al_6O_5 were examined. These results are plotted in figure 4.8. For both clusters the HOMO orbitals are found to be 4 3s orbitals located on the terminal Al atoms. As a result, it is confirmed that the $3s^2$ orbital is occupied. In each case the LUMO is 3p, further confirming that each cluster is monovalent. In the case of Al_6O_4, the LUMO is represented by pi-bonding between the central Al atoms with the next four highest unoccupied orbitals being 3p orbitals located on the 4 four terminal Al atoms. ForAl_6O_5, the LUMO is triply degenerate with all three orbitals being made up of 3p orbitals centered on the terminal Al atoms. Around -2 eV there is a grouping of blue orbitals, these correspond to oxygen lone pairs that are not bonded to Al sites. Bellow that, at roughly -4 eV,

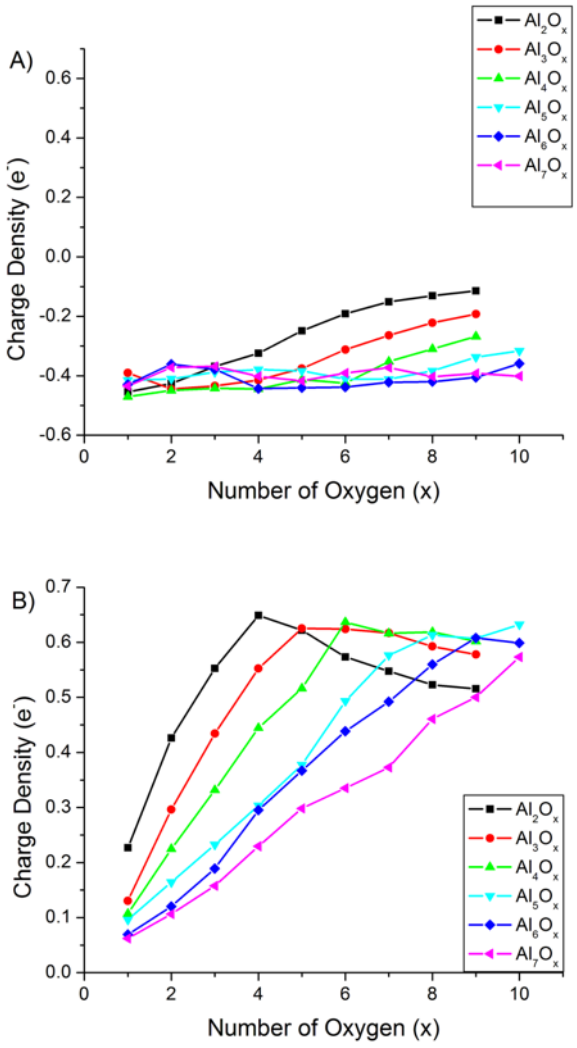

Figure 4.7: A) Hirshfield charge of oxygen. B) Hirshfield charge of aluminum.

there is a set of grey orbitals. These orbitals correspond to mixed orbital between the Al and O atoms. In figure 4.8a there are also two orbitals depicted that show weak pi-bonding inAl_6O_4. These orbitals are orbitals 10 and 11 of which they have a combined 3p occupation of roughly 15. A similar situation is seen in Al_6O_5 in which orbitals 11 and 12 exhibit weak pi-bonding with a combined 3p occupation of around 19. This weak pi-bonding plays an integral part in the planarity of these structures as it is energetically preferable to keep the pi-bonded atoms in plane with one another. Although this provides a good explanation for the planarity of Al_6O_4 and Al_6O_5 it does little to explain the lack of planar structures in the Al_7O_m regime.

In figure 4.9 the ground states for a range of Al_7O_m clusters are shown as well as several low-lying isomers. For both Al_7O_4 and Al_7O_5 there exist near planar structures. The terminal Al atoms are held in plane with respect to their nearest central Al atoms much as in Al_6O_4 and Al_6O_5 but in these cases the Al-Al bonds in the center are bent and as a result destroy the

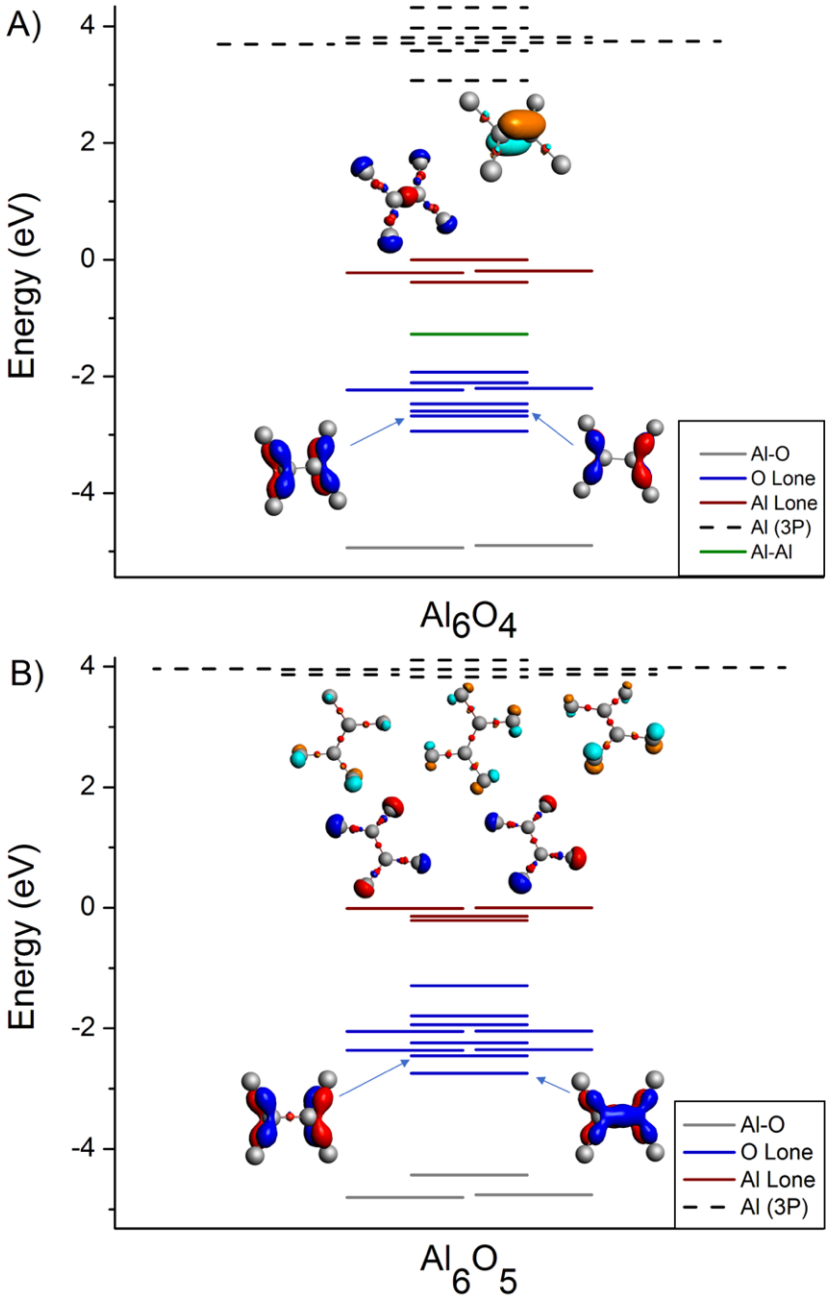

Figure 4.8: Molecular orbitals of Al_6O_4 and Al_6O_5. Continuous lines correspond to filled orbitals while the dashed lines represent unoccupied orbitals.

planarity of these clusters. Unlike the Al_6O_4 case, the central Al atoms exhibit pi-bonding as a result of O atom they are bonded to the Al-Al bond exhibits no such phenomenon and as a result these bonds are free to be bent. It can be seen that in this size regime planar or near planar structures no longer exist in the ground state. This can be explained by examining the ground state structures and realizing the there is a preference for trivalent O. The existence of these trivalent O atoms at this stage implies that there is a tipping point for number of Al atoms at which trivalent O is more efficient than divalent O, thereby eliminating the possibility of planar geometries.

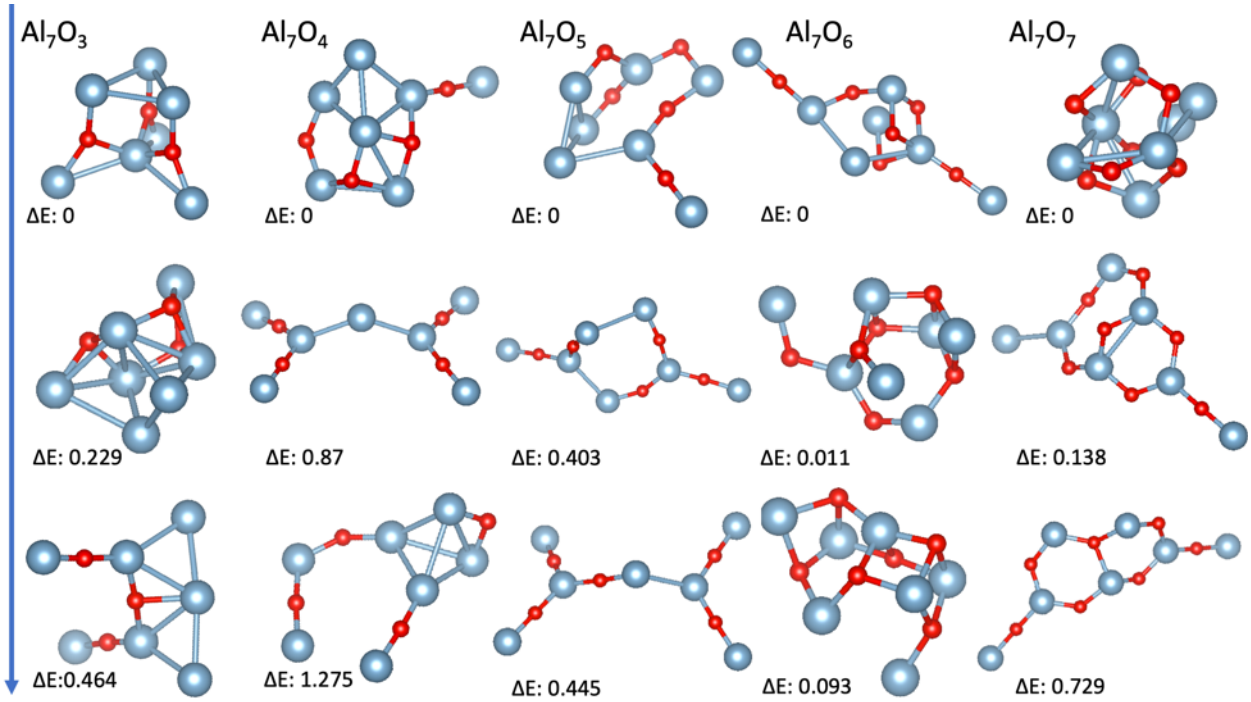

Figure 4.9: Ground state structures and low-lying isomers for $Al_7O_m(3 \leq m \leq 7)$

Chapter 5

Structure of $Al_nO_m^+$

The work done in this section was motived by the mass spectrometry results shown in Figure 5.1. These results are marked by $Al_nO_m^+$ clusters with large intensities that do not correspond to the 2:3 ratio of Al atoms to O atoms that one would expect to see. The spectrometry results brought in to question why such large intensities would exist for what were mostly oxygen rich clusters. To that end the electronic and energetic stability of these clusters as well as a large variety of other $Al_nO_m^+$ structures for of $Al_nO_m^+$ $(2 \leq n \leq 7; 1 \leq m \leq 10)$ were explored. The following results attempt to shed light on

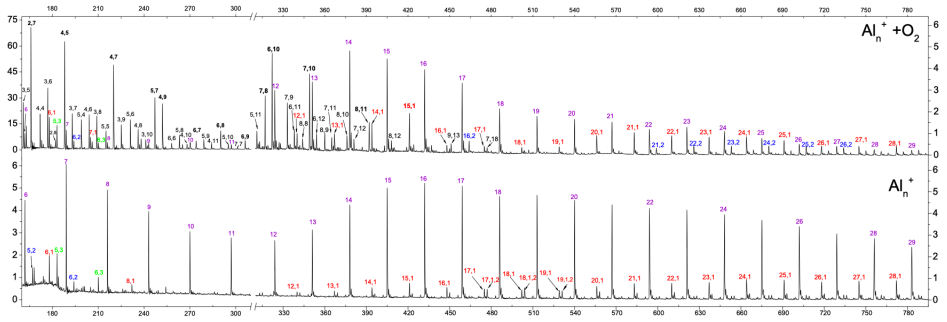

Figure 5.1: A) Mass spectrometry of $Al_nO_m^+$ clusters formed in the presence of large quantities of O_2. B) Mass spectrometry results of bare Al_n^+ clusters.

the existence of these clusters within this experiment as well as their potential to exist outside of a controlled environment.

As with the neutral Al_nO_m clusters, the ground state structures were calculated for clusters with Al from 1 to 7 and O from 1 to 10 and only structures where Al is greater than 2 were considered in regards to electronic structure. The atomic structures of these clusters can be seen in figure 5.2. For $Al_nO_m^+$ clusters the breaking of Al-Al bonds and the insertion of an O atom in its place continues to hold true and can be attributed to the lower binding energy of AlO in comparison to Al_2. As O saturation is reached O-O bonds begin to form and eventually O-O-O bonds. At small sizes $Al_nO_m^+$ clusters exhibit

planar geometries in either linear or ring-shaped forms.

5.1 Electronic Structure of $Al_nO_m^+$

In an effort to understand the energetic stability of $Al_nO_m^+$ clusters the HOMO-LUMO gap, Fragmentation energy and O_2 binding energy were examined. Figure 5.3 shows the HOMO-LUMO gaps for the various $Al_nO_m^+$ clusters. It is generally expected that clusters with closed electronic shells will have large HOMO-LUMO gaps with respect to similar clusters. As neutral Al atoms have a valance of 3 and O atoms a valance of -2 only clusters with even numbers of Al atoms should have closed shells. Being that these clusters are cations, only clusters in which there is an odd number of Al atoms are capable of have a closed electronic shell. In this study Al_3O^+, $Al_3O_4^+$, $Al_5O_3^+$, $Al_5O_7^+$, $Al_7O_{10}^+$ were found to have the greatest HOMO-LUMO gaps. Previous works have shown that for Al_n clusters there is a change in valance associated with site. For smaller clusters with low coordination Al atoms are

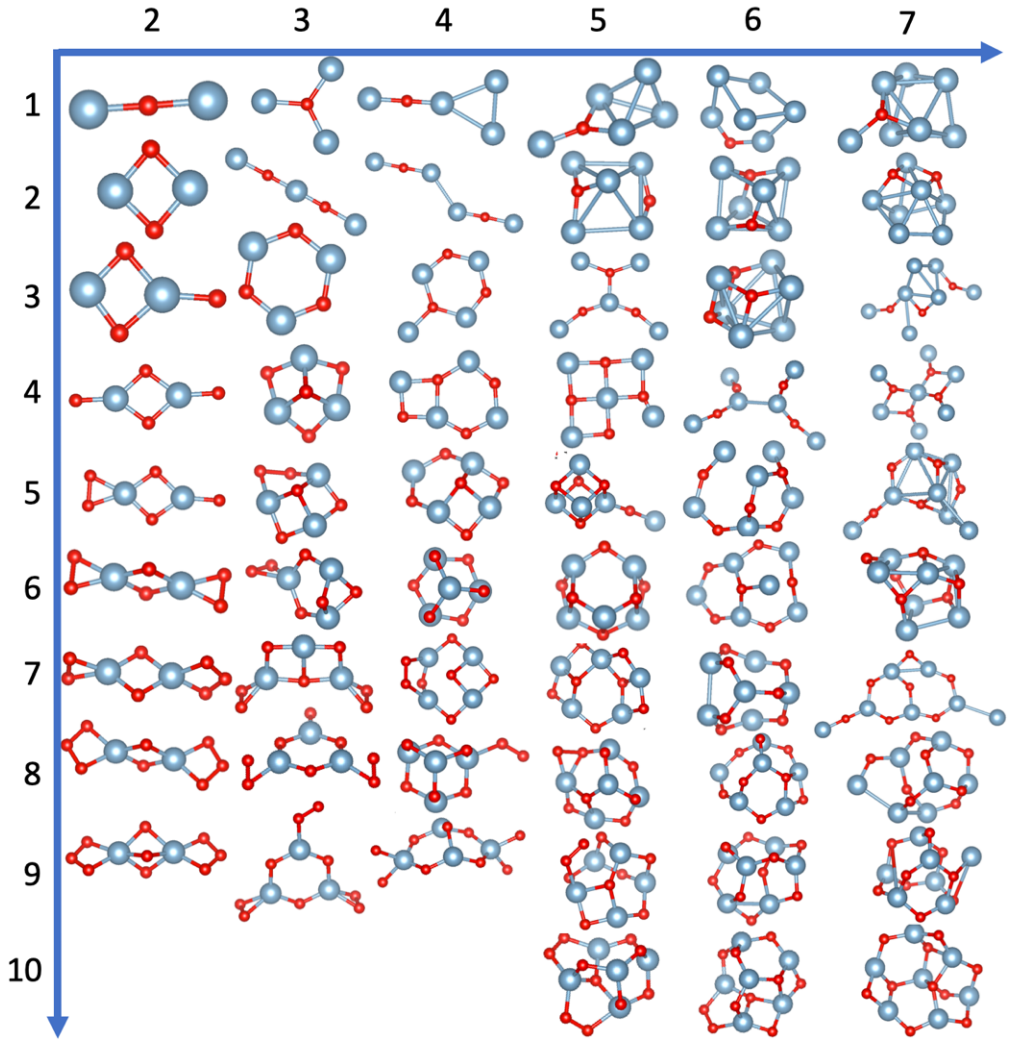

Figure 5.2: . Ground state atomic structures of $Al_nO_m^+(2 \leq n \leq 7; 1 \leq m \leq 10)$. Aluminum is blue, Oxygen is Red.

monovalent, but as the clusters grow in size and coordination increases the Al atoms become trivalent. The monovalent behavior of small clusters then explains the large HOMO-LUMO gap as each Al atom will be in the +1 oxidation state whereas the O atom will be in the -2 oxidation state. As Al_3O^+ has one less electron than the neutral cluster, the result is a closed shell. In the case of $Al_5O_3^+$ the four terminal Al atoms are in the +1 oxidation state and the central Al atom is in the +3 oxidation state. This implies that the terminal Al atoms are lowly coordinated and the central Al atom is highly coordinated. For $Al_3O_4^+$, $Al_5O_7^+$, and $Al_7O_{10}^+$ can be said to have Al atoms which are trivalent and O atoms in the -2 oxidation state. As each of these has one less electron than the neutral cluster would, these three clusters can be said to have a closed electronic shell. This examination implies that at small sizes the electronic stability is dependent upon the multiple valance of the Al sites.

As the calculations in this chapter are in support of experimental results in which clusters undergo multiple

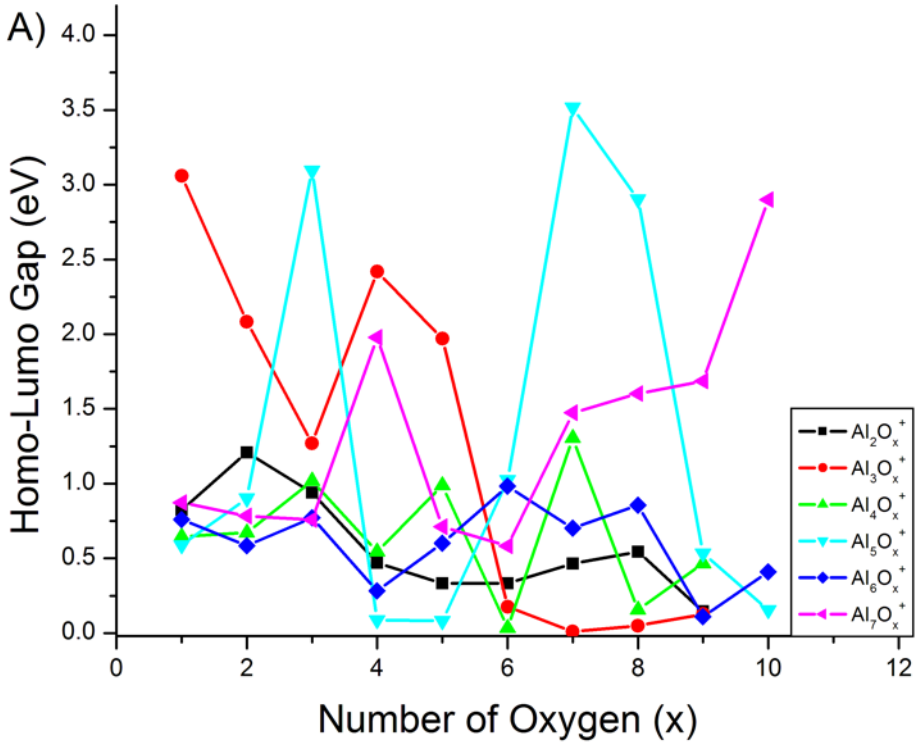

Figure 5.3: HOMO-LUMO gaps of $Al_nO_m^+(2 \leq n \leq 7; 1 \leq m \leq 10)$. B) Fragmentation energy

collisions, special consideration must be taken in regards to the fragmentation energy. The Fragmentation energies for all $Al_nO_m^+$ included in this study are plotted in figure 5.4. The clusters with the greatest fragmentation energies are found to be Al_3O^+, $Al_3O_4^+$, $Al_5O_7^+$, and $Al_7O_{10}^+$. Each of these clusters are found to have Al atoms in the +3 state and O atoms in the -2 state with the exception of Al_3O^+. In the case ofAl_3O^+ the Al atoms are weakly coordinated. This results in Al atoms in the +1 state behaving similarly to more strongly coordinated clusters with Al atoms in the +3 oxidation state. It should be noted that for other cases not including Al_3O^+, the Al to O ratio of these clusters correspond to the 2:3 ratio found in bulk Alumina. Figure 5.4B charts the fragmentation energies as a function of their O/Al ratio, where the fragmentation channel is highlighted by the smallest of the fragments. The most common fragments for $Al_nO_m^+$ clusters were found to be O_2, O, $Al+$, and Al_2O. In the case of oxygen rich clusters, fragmentation channels tend to involve an O_2 or rarely O_3. The fragmentation energies for these clusters were in general

less than three eV. As the O to Al ratio begins to approach 3:2 O and Al^+ fragments dominate. In this range the highest fragmentation energies are seen with most having a value above three eV. As clusters approach the 2:1 ratio the most common fragment becomes Al_2O and the fragmentation energies again drop to below 3 eV. These results support the stability of clusters with an Al to O ratio of 2:3 as clusters in that range have larger fragmentation energies while clusters out of that range tend to fragment in such a way that brings the large fragment closer to this ideal ratio.

Although fragmentation energy has already been used to discuss energetic stability and is a strong metric, O_2 binding energy was also examined. While Al, O, and AlO binding energies were also calculated it was decided that for the purpose of this work O_2 binding energy was the most informative. This is because in the actual experiment that was carried out Al_n^+ clusters were brought into the presence of O_2 molecules to form these clusters. In figure 5.5 it can be seen that the binding energy of $Al_nO_m^+$ clusters decreases as clusters

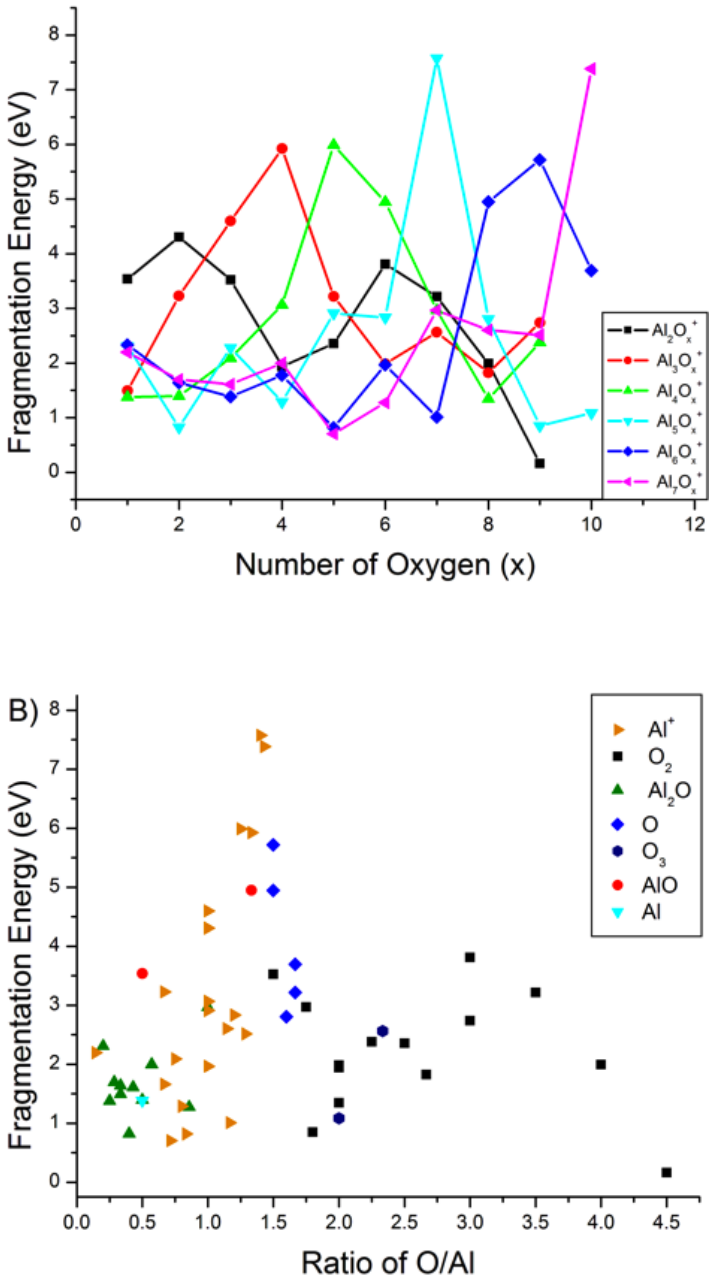

Figure 5.4: A) Fragmentation energy of$Al_nO_m^+$ $(2 \leq n \leq 7; 1 \leq m \leq 10)$ B)Fragmentation energy of $Al_nO_m^+$ $(2 \leq n \leq 7; 1 \leq m \leq 10)$ as a ratio of O/Al with lowest channel represented by smallest fragment.

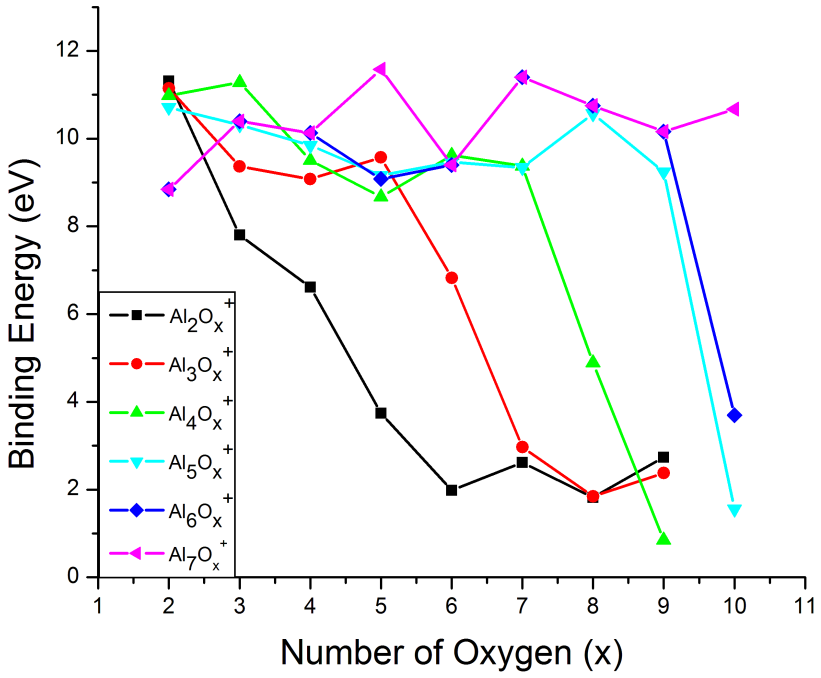

Figure 5.5: O_2 bonding energy of $Al_nO_m^+$ $(2 \leq n \leq 7; 1 \leq m \leq 10)$

approach O saturation. This implies that all O_2 molecules added after this point are only weakly bound to the cluster and as a result the overall stability of these clusters are low. When actual experiments are conducted, $Al_nO_m^+$ production generally involves the removal of an electron from the neutral species of that cluster. As a result, the intensity of an observed species is directly related to the ability to ionize the neutral

species. With this in mind the adiabatic ionization energies of all Al_nO_m clusters in this study were examined. These energies were calculated using Eq. 2.2 in the theoretical methods section. From figure 5.6 it can be seen that there is a drastic variation in the ionization energies for these clusters. Al_2O_m , where m is greater than 5, and Al_3O_8 are composed largely of O_2 andO_3 molecules. As O_2 and O_3 have ionization energies of 12.06 and 12.53 eV, the abundance of these molecules is the listed clusters has the effect of greatly increasing their ionization energies. Al_4O_6 and Al_6O_9 have relatively large ionization energies as well. These ionization energies can be explained as Al_4O_6 and Al_6O_9 correspond to the Al to O ration 2:3 present in bulk Al_2O_3 and as a result have large ionization energies. The lowest energy values present are Al_5O_3, Al_7O_3, and Al_7O_7. Each of these clusters have a large HOMO-LUMO gap and as a result it would not be expected for these clusters to readily ionize.

Figures 5.7A and 5.7B plot the Hirshfield charge on O and Al with respect to cluster size. This data provides an analysis of

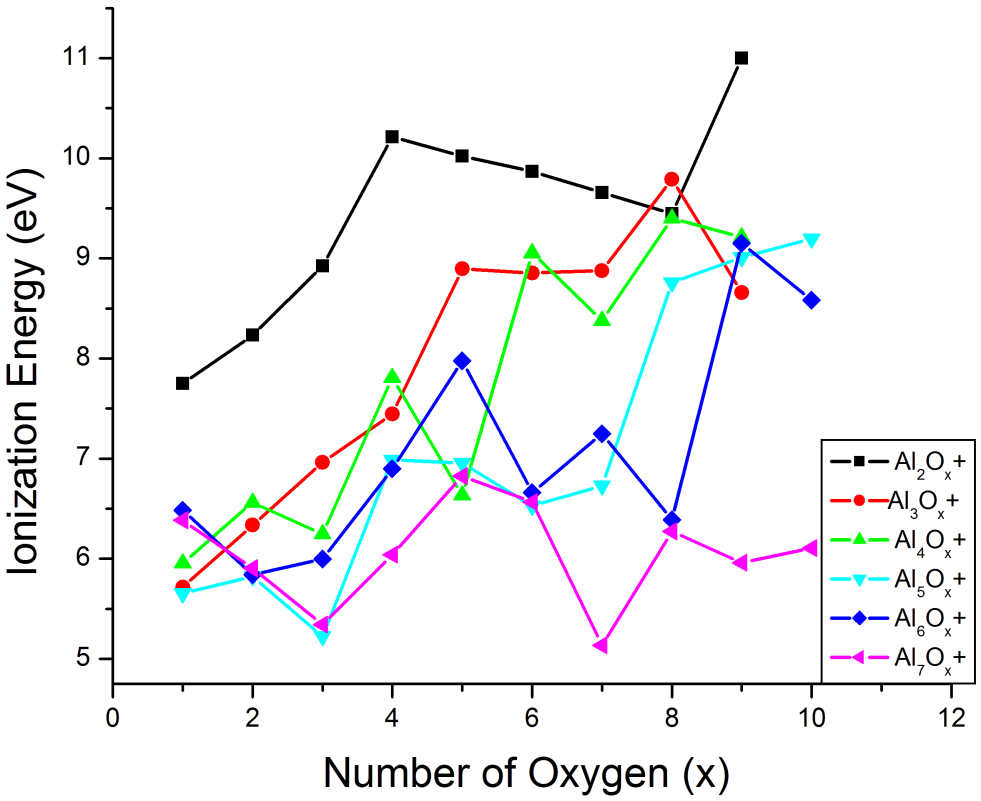

Figure 5.6: Fragmentation energy of of Al_nO_m $(2 \leq n \leq 7; 1 \leq m \leq 10)$

the effects of oxygen coverage on the charge transfer of $Al_nO_m^+$ clusters. For clusters in which the Al to O ratio is less than or equal to approximately 1:2 O has a charge between -0.3 and -0.45. After this point the charge on O drops drastically, signifying O saturation and the formation of O-O bonds. Figure5.7b supports these results as after $Al_2O_3^+$, $Al_3O_4^+$, $Al_4O_6^+$, and $Al_5O_7^+$ there is a monotonic decrease in charge on Al sites. Although these results generally align well with the results of the neutral structures and also aligns with the ratio of Al to O in bulk Alumina there is one stark difference. Unlike the neutral species the saturation point does not correspond to a set charge across cluster sizes. In fact, this number decreases as the size of the cluster grows, implying that the charge representing the +3 oxidation state changes with regards to size in charged clusters.

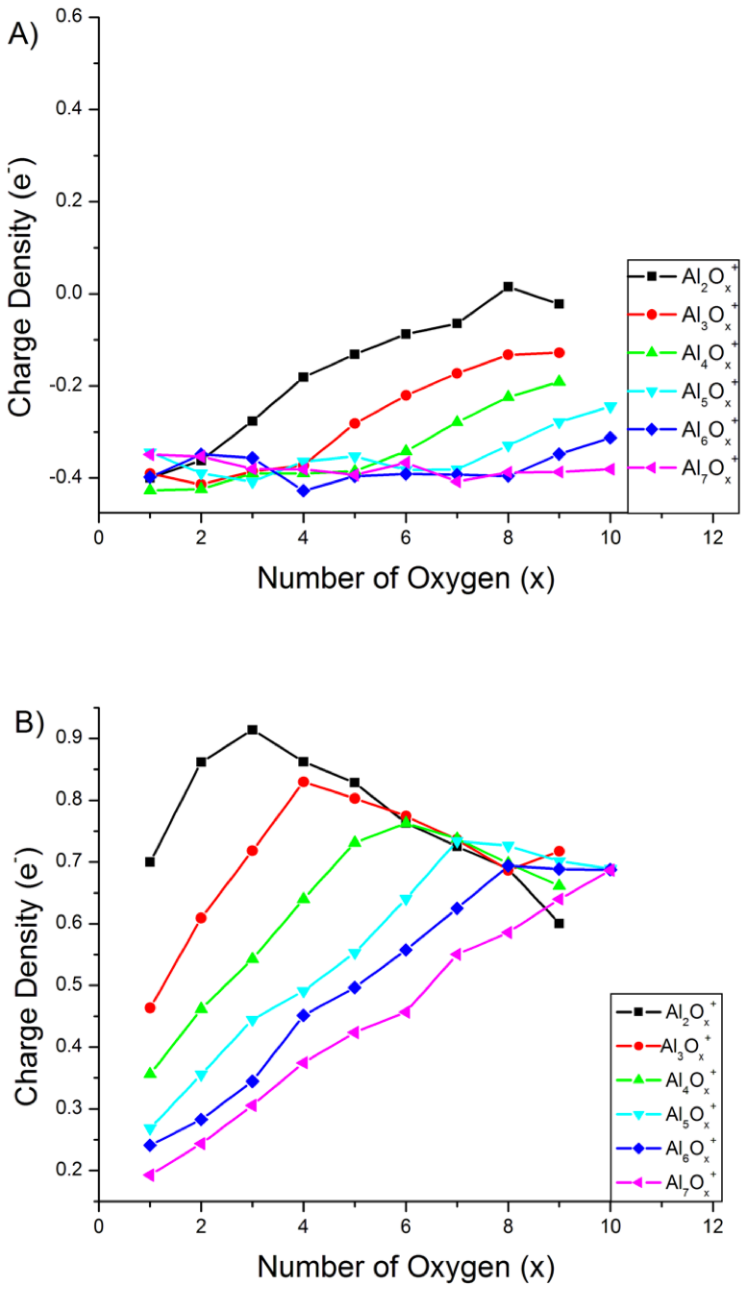

Figure 5.7: A) Hirshfield charge density of oxygen. B) Hirshfield charge density of aluminum.

5.2 Results in Relation to Experiment

An important result of this study is to gather an understanding of the stability of $Al_nO_m^+$ clusters in general as well as the clusters represented in figure 5.8. Figure 5.8 gives the structures of the 12 clusters with the most intense peaks found in the experiment. From this figure it can be seen that with the exception of $Al_7O_m^+$ clusters all are O rich and most O-O bonds or multiple O free radicals. Of these selected clusters only $Al_5O_7^+$ and $Al_7O_{10}^+$, both of which correspond to the ideal 2:3 ratio, have large HOMO-LUMO gaps. All of the remaining clusters have HOMO-LUMO gaps that are below average implying that these structures are not chemically stable. In regards to fragmentation energy, again, only $Al_5O_7^+$ and $Al_7O_{10}^+$ have large values while all other clusters are roughly average. As these clusters show signs of being chemically reactive and relatively easy to fragment it does not seem that they would be stable. If the number of collisions between the Al vapor and the O_2 gas were kept relatively low

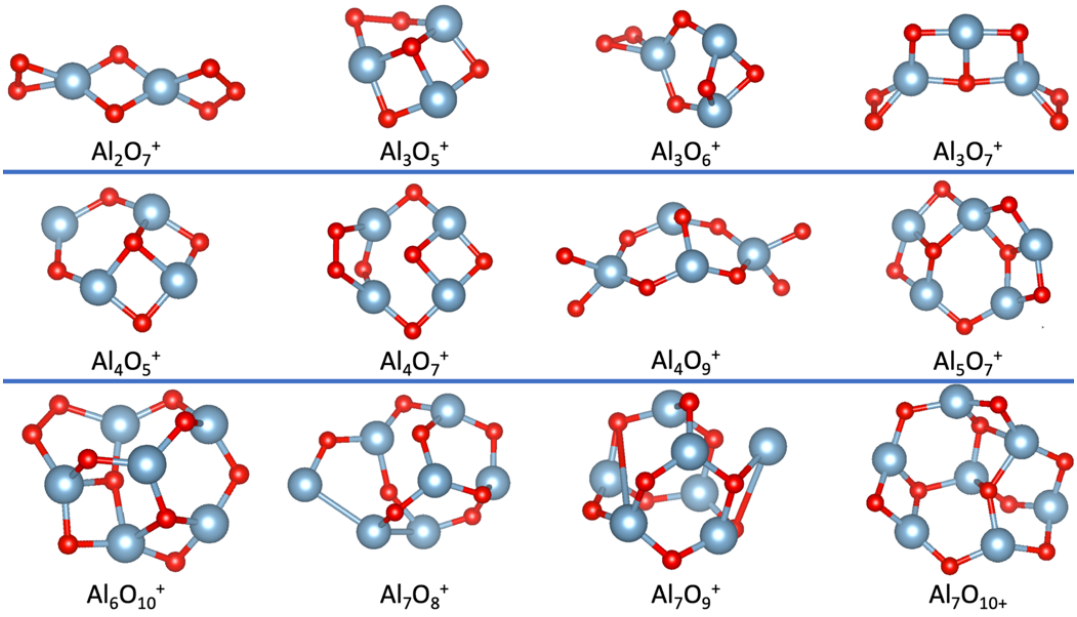

Figure 5.8: Structures found experimentally

one would expect to see clusters such as these were there is essentially O_2 molecules loosely binding to Al_n^+ clusters before experiencing enough collision to be fragmented.

Chapter 6

Conclusions

6.1 Summary and Future Projects

This work focused on the atomic and electronic structure of Al_nO_m and $Al_nO_m^+$ clusters with n ranging from 2-7 atoms and m from 1-10. Examination of this clusters was undertaken to gain insight into the various ways in which small Al_nO_m clusters form. The results of this work support the idea that from an energetic standpoint small aluminum oxide clusters are most stable when the ratio of Al to O is 2:3. Although, Al_nO_m structures conforming to this ratio are indeed the most common way to achieve energetic stability it has been shown

that there is another route by which this can be achieved. Clusters such as Al_4O_4, Al_5O_3, Al_6O_4, and Al_6O_5 have large HOMO-LUMO gaps indicative of chemical stability. This stability is the result of multiple valance in regards to the Al atoms of each cluster. These clusters are marked by terminal Al atoms that are monovalent and also in the +1 oxidation state. When paired with central Al atoms that are trivalent these clusters form closed electronic shells.

In regards to $Al_nO_m^+$ clusters, no such multiple valence structures were found. Clusters in which this behavior is seen have a preference for planar geometries with terminal Al atoms, a scenario that was uncommon in $Al_nO_m^+$. It was also found that although oxygen rich $Al_nO_m^+$ clusters can be created the energetic stability of such clusters is mediocre at best. As a result, if these clusters where to exist in a high collision environment one would expect them to fragment in to more stable clusters closer to the 2:3 ratio.

In the future it would be of interest expand this study to include clusters with higher numbers of atoms as well as

$Al_nO_m^-$ clusters. Doing such would allow for a greater understanding of multiple valance in regards to size constraints as well as bonding.

References

[1] P Andre Clayborne, Olga Lopez-Acevedo, Robert L Whetten, Henrik Grönbeck, and Hannu Häkkinen. Evidence of superatom electronic shells in ligand-stabilized aluminum clusters. *The Journal of chemical physics*, 135(9):094701, 2011.

[2] Zahra Badri, Shubhrodeep Pathak, Heike Fliegl, Parviz Rashidi-Ranjbar, Radovan Bast, Radek Marek, Cina Foroutan-Nejad, and Kenneth Ruud. All-metal aromaticity: revisiting the ring current model among transition metal clusters. *Journal of chemical theory and computation*, 9(11):4789–4796, 2013.

[3] Axel D Becke. Density-functional exchange-energy approx-

imation with correct asymptotic behavior. *Physical review A*, 38(6):3098, 1988.

[4] Axel D Becke. Density-functional thermochemistry. iii. the role of exact exchange. *The Journal of chemical physics*, 98(7):5648–5652, 1993.

[5] Ulrich Boesl. Time-of-flight mass spectrometry: introduction to the basics. *Mass spectrometry reviews*, 36(1):86–109, 2017.

[6] Alexander I Boldyrev and Lai-Sheng Wang. All-metal aromaticity and antiaromaticity. *Chemical reviews*, 105(10):3716–3757, 2005.

[7] Ralf Burgert, Hansgeorg Schnöckel, Andrej Grubisic, Xiang Li, Sarah T Stokes, Kit H Bowen, GF Ganteför, Boggavarapu Kiran, and Purusottam Jena. Spin conservation accounts for aluminum cluster anion reactivity pattern with o2. *Science*, 319(5862):438–442, 2008.

[8] Ujjal Das and Krishnan Raghavachari. Al–h bond formation in hydrated aluminum oxide cluster anions, 2006.

[9] Ujjal Das and Krishnan Raghavachari. Al5o4: A superatom with potential for new materials design. *Journal of chemical theory and computation*, 4(12):2011–2019, 2008.

[10] Samantha DeCarlo, Dennis H Mayo, Warren Tomlinson, Junkai Hu, Joseph Hooper, Peter Zavalij, Kit Bowen, Hansgeorg Schnockel, and Bryan Eichhorn. Synthesis, structure, and properties of al (rbpy) 3 complexes (r= t-bu, me): Homoleptic main-group tris-bipyridyl compounds. *Inorganic chemistry*, 55(9):4344–4353, 2016.

[11] A Ecker, E Weckert, and H Schnöckel. Synthesis and structural characterization of an ai77 cluster. *Nature*, 387(6631):379, 1997.

[12] David Gobrecht, Leen Decin, Sergio Cristallo, and Stefan T Bromley. A global optimisation study of the low-lying iso-

mers of the alumina octomer (al2o3) 8. *Chemical Physics Letters*, 711:138–147, 2018.

[13] YongBing Gu, NaiXiao Xu, MengHai Lin, and Kai Tan. Structures, stabilities and properties of hollow (al2o3) n clusters (n= 10, 12, 16, 18, 24 and 33): Studied with density functional theory. *Computational and theoretical chemistry*, 1063:29–34, 2015.

[14] Jihane Hankache and Oliver S Wenger. Organic mixed valence. *Chemical reviews*, 111(8):5138–5178, 2011.

[15] Alexander Heckmann and Christoph Lambert. Organic mixed-valence compounds: a playground for electrons and holes. *Angewandte Chemie International Edition*, 51(2):326–392, 2012.

[16] Patrick Henke, Nils Trapp, Christopher E Anson, and Hansgeorg Schnöckel. Al12k8 [oc (ch3) 3] 18: a wade, zintl, or metalloid cluster, or a hybrid of all three? *Angewandte Chemie*, 122(18):3214–3218, 2010.

[17] Xiani Huang, Tong Gao, Xiaole Pan, Dong Wei, Chunju Lv, Laishun Qin, and Yuexiang Huang. A review: Feasibility of hydrogen generation from the reaction between aluminum and water for fuel cell applications. *Journal of Power Sources*, 229:133–140, 2013.

[18] Yeon Soo Kim, GL Hofman, AB Robinson, JL Snelgrove, and N Hanan. Oxidation of aluminum alloy cladding for research and test reactor fuel. *Journal of Nuclear Materials*, 378(2):220–228, 2008.

[19] Walter Kohn and Lu Jeu Sham. Self-consistent equations including exchange and correlation effects. *Physical review*, 140(4A):A1133, 1965.

[20] Xénophon Krokidis, Pascal Raybaud, Anne-Elisabeth Gobichon, Bernadette Rebours, Patrick Euzen, and Hervé Toulhoat. Theoretical study of the dehydration process of boehmite to γ-alumina. *The Journal of Physical Chemistry B*, 105(22):5121–5130, 2001.

[21] Aleksey E Kuznetsov, K Alexander Birch, Alexander I Boldyrev, Xi Li, Hua-Jin Zhai, and Lai-Sheng Wang. All-metal antiaromatic molecule: Rectangular al44-in the li3al4-anion. *Science*, 300(5619):622–625, 2003.

[22] Xi Li, Aleksey E Kuznetsov, Hai-Feng Zhang, Alexander I Boldyrev, and Lai-Sheng Wang. Observation of all-metal aromatic molecules. *Science*, 291(5505):859–861, 2001.

[23] Yang Li, Jie Xiao, Tatyana E Shubina, Min Chen, Ziliang Shi, Martin Schmid, Hans-Peter Steinruck, J Michael Gottfried, and Nian Lin. Coordination and metalation bifunctionality of cu with 5, 10, 15, 20-tetra (4-pyridyl) porphyrin: toward a mixed-valence two-dimensional coordination network. *Journal of the American Chemical Society*, 134(14):6401–6408, 2012.

[24] Feng Lu, JianZhou Zhao, Hongming Weng, Zhong Fang, and Xi Dai. Correlated topological insulators with mixed valence. *Physical review letters*, 110(9):096401, 2013.

[25] Alexandre L Magalhães. Gaussian-type orbitals versus slater-type orbitals: A comparison. *Journal of Chemical Education*, 91(12):2124–2127, 2014.

[26] NF Mott. A theory of the formation of protective oxide films on metals. *Transactions of the faraday Society*, 35:1175–1177, 1939.

[27] Sven Neukermans, Nele Veldeman, Ewald Janssens, Peter Lievens, Z Chen, and PVR Schleyer. Combined experimental and theoretical study of small aluminum oxygen clusters. *The European Physical Journal D*, 45(2):301–308, 2007.

[28] John P Perdew, Kieron Burke, and Matthias Ernzerhof. Generalized gradient approximation made simple. *Physical review letters*, 77(18):3865, 1996.

[29] Amol B Rahane, Mrinalini D Deshpande, and Vijay Kumar. Structural and electronic properties of (al2o3) n clusters with n= 1–10 from first principles calculations. *The Journal of Physical Chemistry C*, 115(37):18111–18121, 2011.

[30] Arthur C Reber, Shiv N Khanna, Patrick J Roach, W Hunter Woodward, and AW Castleman Jr. Reactivity of aluminum cluster anions with water: origins of reactivity and mechanisms for h2 release. *The Journal of Physical Chemistry A*, 114(20):6071–6081, 2010.

[31] J Ulises Reveles, SN Khanna, PJ Roach, and AW Castleman. Multiple valence superatoms. *Proceedings of the National Academy of Sciences*, 103(49):18405–18410, 2006.

[32] Constantin Romanescu, Timur R Galeev, Wei-Li Li, Alexander I Boldyrev, and Lai-Sheng Wang. Transition-metal-centered monocyclic boron wheel clusters (m© b n): a new class of aromatic borometallic compounds. *Accounts of chemical research*, 46(2):350–358, 2012.

[33] David Sholl and Janice A Steckel. *Density functional theory: a practical introduction*. John Wiley & Sons, 2011.

[34] Fangyuan Song, Yong Ding, Baochun Ma, Changming Wang, Qiang Wang, Xiaoqiang Du, Shao Fu, and Jie Song.

K 7 [co iii co ii (h 2 o) w 11 o 39]: a molecular mixed-valence keggin polyoxometalate catalyst of high stability and efficiency for visible light-driven water oxidation. *Energy & Environmental Science*, 6(4):1170–1184, 2013.

[35] G t Te Velde, F Matthias Bickelhaupt, Evert Jan Baerends, C Fonseca Guerra, Stan JA van Gisbergen, Jaap G Snijders, and Tom Ziegler. Chemistry with adf. *Journal of Computational Chemistry*, 22(9):931–967, 2001.

[36] RP Turco, RC Whitten, and OB Toon. Stratospheric aerosols: Observation and theory. *Reviews of Geophysics*, 20(2):233–279, 1982.

[37] G Van Harten, F Snik, and CU Keller. Polarization properties of real aluminum mirrors, i. influence of the aluminum oxide layer. *Publications of the Astronomical Society of the Pacific*, 121(878):377, 2009.

[38] E v Van Lenthe, JG Snijders, and EJ Baerends. The zero-order regular approximation for relativistic effects: The ef-

fect of spin–orbit coupling in closed shell molecules. *The Journal of chemical physics*, 105(15):6505–6516, 1996.

[39] Erik van Lenthe, Andreas Ehlers, and Evert-Jan Baerends. Geometry optimizations in the zero order regular approximation for relativistic effects. *The Journal of chemical physics*, 110(18):8943–8953, 1999.

[40] PR Willmott and JR Huber. Pulsed laser vaporization and deposition. *Reviews of Modern Physics*, 72(1):315, 2000.

[41] Jin Zhang and Anastassia N Alexandrova. Double σ-aromaticity in a surface-deposited cluster: Pd4 on tio2 (110). *The journal of physical chemistry letters*, 3(6):751–754, 2012.

[42] Qiyao Zhang and Longjiu Cheng. Structural determination of (al2o3) n (n= 1–15) clusters based on graphic processing unit. *Journal of chemical information and modeling*, 55(5):1012–1020, 2015.

[43] Xinxing Zhang, Bryan Eichhorn, Hansgeorg Schnöckel, and Kit Bowen. The al (i) molecule, ph2coal and its anion. *Chemical Physics Letters*, 659:36–39, 2016.

[44] Xinxing Zhang, Gerd Ganteför, Bryan Eichhorn, Dennis Mayo, William H Sawyer, Ann F Gill, Anil K Kandalam, Hansgeorg Schnöckel, and Kit Bowen. Low oxidation state aluminum-containing cluster anions: Cp alnh-, n= 1–3. *The Journal of chemical physics*, 145(7):074305, 2016.